LBL--27584

DE90 000138

High Resolution Photoelectron Spectroscopy of Clusters of Group V Elements

Lai-sheng Wang, B. Niu, Y.T. Lee and D.A. Shirley

Department of Chemistry, University of California
and Materials and Chemical Sciences Division
Lawrence Berkeley Laboratory, 1 Cyclotron Road
Berkeley, CA 94720 (U.S.A.)

MASTER

DISTRIBUTION OF THIS DOCUMENT IS UNLIMITED

Abstract

High resolution HeI (580Å) photoelectron spectra of As_2, As_4 and P_4 were obtained with a newly-built high temperature molecular beam source. Vibrational structure was resolved in the photoelectron spectra of the three cluster species. The Jahn-Teller effect is discussed for the ^2E and $^2T_2$ states of P_4^+ and As_4^+. As a result of the Jahn-Teller effect, the ^2E state splits into two bands, and the $^2T_2$ state splits into three bands, in combination with the spin-orbit effect. It was observed that the ν_2 normal vibrational mode was involved in the vibronic interaction of the ^2E state, while both the ν_2 and ν_3 modes were active in the $^2T_2$ state.

1. Introduction

Clusters bridge the gap between isolated atoms and molecules on one hand and condensed matter on the other. Research on clusters has received great attention in recent years [1]. One central question in cluster research is the change of electronic properties as a function of cluster size. Photoelectron spectroscopy should be a powerful technique in this study, because it probes directly the electron energy levels of matter. However, a difficulty in applying photoelectron spectroscopy to cluster systems is need for size-selectivity. As a result, much of the effort in studying the electronic structure of clusters has been focused on the photodetachment of negatively-charged clusters [2,3]. We are only beginning to see photoemission studies on size-selected neutral clusters [4].

We are interested in the high resolution photoelectron spectroscopy of neutral clusters. A high temperature molecular beam source has recently been built to study neutral clusters and other high temperature species [5]. The Group V elements were chosen for our initial study because they provide an easy solution for the size-selectivity. The vapor phases of these elements are mainly composed of tetramers for P, As, and Sb, and dimers and atomic species for Bi [6]. Diatomics of P, As, and Sb can be produced by pyrolyzing the tetramers [7], or by evaporating appropriate compounds of these elements [8]. Low resolution HeI photoelectron spectra of P_2 [7,9,10], P_4 [10-12], As_2 [13,14], As_4 [13,14] and Sb_4 [15,16] have been reported before. In this paper, we present the high resolution HeI photoelectron spectra of As_2, As_4, and P_4. Vibrational structure was resolved for all three species, allowing us to do more detailed analyses on the spectroscopy of the final states. Especially for the ^2E and $^2T_2$ states of P_4^+ and As_4^+, the vibrational analyses enable us to gain insight into the Jahn-Teller effect.

2. Experimental

The photoelectron spectrometer [17] and the high temperature molecular beam source [5] have been described in detail elsewhere. Only a brief description is given here. The spectrometer consists of the beam source, a rare gas discharge lamp, a quadrupole mass spectrometer and a hemispherical electron energy analyzer with a multichannel detector.

The high temperature molecular beam source used electron bombardment heating and graphite crucibles with carrier gas entrainment. The experimental conditions are shown in Table I. All the samples were commercially available from CERAC.

Either Ar or Xe was usually used as a calibration gas. The energy resolution, as measured for the Ar^+ $^2P_{3/2}$ peak, was about 13 meV.

3. Results and discussion

3.1 As_2

The As_2 spectrum is shown in Fig. 1. The valence electronic configuration of As_2 can be described as $1\sigma_g^2 1\sigma_u^2 2\sigma_g^2 1\pi_u^4$. Ionization of the $1\pi_u$ orbital results in the $^2\Pi_u$ band in As_2^+, which is split by the spin-orbit effect. The removal of a $2\sigma_g$ electron gives rise to the sharp $^2\Sigma_g^+$ band with little vibrational excitation. Extensive vibrational structure was observed for the $^2\Pi_{u3/2}$ and $^2\Pi_{u1/2}$ bands, which are partially overlapped. This makes it difficult to assign exactly where the $^2\Pi_{u1/2}$ band starts. From the assignments given in Fig. 1, vibrational frequencies of 360 cm^{-1} and 450 cm^{-1} were derived for the $^2\Pi_{u1/2}$ and $^2\Pi_{u3/2}$ states, respectively. In light of the bonding character of the $1\pi_u$ orbital, a vibrational frequency of 450 cm^{-1} for the $^2\Pi_{u3/2}$ state is surprising, because it is even larger than that of the neutral ground state (429 cm^{-1} [18]). Furthermore, the large difference between the vibrational frequencies of the two spin-orbit states is also unexpected. A similar situation has been encountered in the $^2\Pi_{u1/2}$ and $^2\Pi_{u3/2}$ states of Br_2^+, which was found to be caused by an avoided curve crossing of the $^2\Pi_{u1/2}$ state from a relativistic CI calculation [19]. Such a calculation is underway for As_2^+ to explain our observation [20]. The experimentally-derived spectroscopic constants for As_2^+ are listed in Table II.

3.2 P_4 and As_4

The vibrationally-resolved spectra of P_4 and As_4 are shown in Figs. 2 and 3, respectively. These two molecules are isoelectronic and have the same tetrahedral geometry. Thus, the two spectra are very similar, with the P_4 spectra being better resolved. The valence electronic configuration of P_4 and As_4 can be written as $(1a_1)^2(1t_2)^6(2a_1)^2(2t_2)^6(1e)^4$, where the $1a_1$ and $1t_2$ orbitals are mainly of the valence s character and the $2a_1$, $2t_2$, and 1e orbitals are primarily composed of the valence p character. As shown in Figs. 2 and 3, only the ionizations of the outermost three orbitals were observed.

Before analyzing the spectra, it is instructive to consider the normal vibrational modes and frequencies of the neutral molecules. For a tetrahedral M_4 molecule, there are three normal modes of vibration, which are listed in Table III for P_4 and As_4 [21].

The $(2a_1)^{-1}$ band in each spectrum consists of a well-resolved vibrational progression. Both from symmetry consideration and from the observed spacings, this progression should be the ν_1 vibrational progression. The frequencies are 560 cm^{-1} and 350 cm^{-1} for P_4^+ and As_4^+, respectively. The $(2t_2)^{-1}$ and $(1e)^{-1}$ bands are much more complicated because of the Jahn-Teller effect, which is discussed in the next section.

3.3 The Jahn-Teller effect

The Jahn-Teller theorem states that highly symmetrical molecular configurations in degenerate electronic states are unstable with respect to certain asymmetric vibrations [22], which carry the nuclei over into distorted configurations and lift the electronic degeneracies. The Jahn-Teller effect is often important for small clusters, because electronic degeneracy is very common in these systems [23,24]. It dictates the geometrical and electronic structures of these species.

In discussing the Jahn-Teller problem, it is essential to know which asymmetrical vibrational modes are active in the vibronic coupling when more than one Jahn-Teller active vibrational mode is present. Ionization of an electron from a 1e orbital would produce a ^2E state, for which only the $\nu_2(e)$ mode is active [25]. Removal of an electron from a $2t_2$ orbital would give rise to a $^2T_2$ state, for which both the $\nu_2(e)$ and the $\nu_3(t_2)$ modes can be involved [25]. Furthermore, spin-orbit splitting is also possible in the $^2T_2$ state.

Expanded spectra of the $(1e)^{-1}$ and $(2t_2)^{-1}$ bands are shown in Figs. 4 and 5 for P_4^+ and As_4^+, respectively. Vibrational structure was partially resolved in these two bands for P_4^+, but not as well for the As_4^+ spectrum due to its smaller vibrational frequencies. Fortunately, the understanding of the P_4^+ spectrum should be sufficient for this series of tetramers. It can be seen from Fig. 4 that the $(1e)^{-1}$ band of P_4^+ is split into two bands, one peaking at ~9.4 eV and the other at ~9.9 eV. The observed vibrational frequencies are 310 cm^{-1} for the first band and 270 cm^{-1} for the second. These values are close to the ground state ν_2 vibrational frequency (Table III). The $(1e)^{-1}$ band of As_4^+ closely resembles that of P_4^+. The Jahn-Teller splitting energies are almost identical (~0.5 eV).

The $(2t_2)^{-1}$ band of As_4^+ was assigned previously to only two spin-orbit split components [14]. As can be seen from Figs. 4 and 5, this band is composed of three components, indicating that the Jahn-Teller effect is also important. Comparing the $(2t_2)^{-1}$ bands of P_4^+, As_4^+, and Sb_4^+ [26] indicates that the separation between the lowest energy component and the two components at higher energies increases from P_4^+ to Sb_4^+, suggesting that the lowest energy component is due to the spin-orbit splitting. Well-resolved vibrational structure was observed for this component in P_4^+. The vibrational frequency is 400 cm^{-1}, consistent with the ν_3 vibrational mode. The two components at higher energy should be due to the Jahn-Teller effect. No simple vibrational progression was observed for any of these components in P_4^+, meaning that both the ν_2 and the ν_3 modes are active in the vibronic interaction.

P_4 and As_4 are simple examples of tetrahedral clusters. The elucidation of the Jahn-Teller effect in these simple systems may help us understand more complicated M_4 clusters.

4. Conclusion

In summary, we have obtained high resolution photoelectron spectra for three Group V element clusters, As_2, As_4, and P_4. Vibrational structure was resolved for the three molecules and vibrational frequencies were derived for the final ionic states. It was found that the vibrational frequencies of the $^2\Pi_{u1/2}$ and $^2\Pi_{u3/2}$ states of As_2^+ are surprisingly different. Very well resolved vibrational spectra were obtained for the $(2a_1)^{-1}$ bands of P_4 and As_4. The Jahn-Teller effect was found to be important in both the $(1e)^{-1}$ and $(2t_2)^{-1}$ bands of these clusters. Both the ν_2 and ν_3 normal modes are active in the vibronic interaction of the $(2t_2)^{-1}$ band.

Acknowledgement

This work was supported by the Director, Office of Energy Research, Office of Basic Energy Sciences, Chemical Sciences Division of the U.S. Department of Energy under the Contract No. DE-AC03-76SF00098.

References

1. See for example, *a.* Kappes, M.M., Chem. Rev. 88, 369 (1988); *b.* Chem. Rev. 86, 491-635 (1986), special issue on 'gas-phase clusters'; *c.* Martin, T.P., Phys. Rep. 95, 167 (1983).
2. Ervin, K.M., Ho, J., and Lineberger, W.C., J. Chem. Phys. 89, 4514 (1988).
3. Cheshnovsky, O., Yang, S.H., Pettiette, C.C., Craycraft, M.J., and Smalley, R.E., Rev. Sci. Instrum. 58, 2131 (1987).
4. Ebehardt, W., Fayet, P., Cox, D., Fu, Z., Kaldor, A., and Sondericker, D., Phsica Scripta, the current issue, (19xx).
5. Wang, L.S., Reutt-Robey, J.E., Niu, B., Lee, Y.T., and Shirley, D.A., in Proceedings of the Fourth International Conference on Electron Spectroscopy, July 10-14, 1989, Honolulu, U.S.A., J. Electron Spectrosc. Relat. Phenom., in press.
6. Nesmeyanov, A.N., Gary, R. (Ed.), Vapor Pressure of the Chemical Elements, p. 286-306, Elsevier, Amsterdam, 1959.
7. Bulgin, D.K., Dyke, J.M., and Morris, A., J. Chem. Soc. Faraday Trans. 2 72, 2225 (1976).
8. Dyke, J.M., Elbel, S., Morris, A., and Stevens, J.C.H., J. Chem. Soc. Faraday Trans. 2 82, 637 (1986).
9. Potts, A.W., Glen, K.G., and Price, W.C., Faraday Discuss. Chem. Soc. 54, 65 (1972).
10. Bock, H. and Muller, H., Inorg. Chem. 23, 4365 (1984).
11. Evans, S., Joachim, P.J., Orchard, A.F., and Turner, D.W., Int. J. Mass Spectrom. Ion Phys. 9, 41 (1972).
12. Brundle, C.R., Kuebler, N.A., Robin, M.B., and Basch, H., Inorg. Chem. 11, 20 (1972).
13. Elbel, S., Dieck, H.T., Walther, H., and Krizek, J., Inorg. Chim. Acta 53, L101

(1981).

14. Dyke, J.M., Elbel, S., Morris, A., and Stevens, J.C.H., J. Chem. Soc. Faraday Trans. 2 82, 637 (1986).
15. Elbel, S., Kudnig, J., Grodzicki, M., and Lempka, H.J., Chem. Phys. Lett. 109, 312 (1984).
16. Dyke, J.M., Morris, A., and Stevens, J.C.H., Chem. Phys. 102, 29 (1986).
17. Pollard, J.E., Trevor, D.J., Lee, Y.T., and Shirley, D.A., Rev. Sci. Instrum. 52, 1837 (1981).
18. Huber, K.P. and Herzberg, G., Spectroscopic Constants of Diatomics, Van Nostrand Reinhold, New York, 1979.
19. Balasubramanian, K., Chem. Phys. 119, 41 (1988).
20. Balasubramanian, K., private communication.
21. Bondybey, V.E., Schwartz, G.P., and Griffiths, J.E., J. Mol. Spectrosc. 89, 328 (1981).
22. Jahn, H.A. and Teller, E., Proc. Roy. Soc. A 161, 20 (1937).
23. Gerber, W.H. and Schumacher, E., J. Chem. Phys. 69, 1692 (1978).
24. Morse, M.D., Hopkins, J.B., Langridge-Smith, P.R.A., and Smalley, R.E., J. Chem. Phys. 79, 5316 (1983).
25. Herzberg, G., Molecular Spectra and Molecular Structure: III. Electronic Spectra and Electronic Structure of Polyatomic Molecules, p. 50, Van Nostrand Reinhold, New York, 1966.
26. Wang, L.S., Lee, Y.T., and Shirley, D.A., to be published.

Table I. Experimental conditions

	T (K)[a]	P (torr)[b]	ϕ (mm)[c]	Starting materials
As_2	~1400	350 (Ne)	0.13	Cu_3As
As_4	~650	200 (He)	0.16	Pure arsenic
P_4	~620	500 (He)	0.16	Red phosphorus

a. Oven temperature ± 50K.

b. Carrier gas pressure.

c. Nozzle diameter.

Table I. Spectroscopic constants of As_2^+.

	$^2\Pi_{u3/2}$	$^2\Pi_{u1/2}$	$^2\Sigma_g^+$
IPad (eV)[a]	9.511(6)	(9.903)	10.228(5)
ω_e (cm^{-1})	450	360	390

a. Adiabatic ionization potential.

Table III. Normal modes of vibration of P_4 and As_4 from Ref. [21].

	$\nu_1(a_1)$	$\nu_2(e)$	$\nu_3(t_2)$
P_4	600 cm^{-1}	360 cm^{-1}	450 cm^{-1}
As_4	340 cm^{-1}	200 cm^{-1}	250 cm^{-1}

Figure captions

Figure 1. HeI photoelectron spectrum of As_2.

Figure 2. HeI photoelectron spectrum of P_4.

Figure 3. HeI photoelectron spectrum of As_4.

Figure 4. The $(1e)^{-1}$ and $(2t_2)^{-1}$ bands of P_4. The three peaks underneath the $(2t_2)^{-1}$ band indicate the three components in this band. They are three voigt functions used to fit the band.

Figure 5. The $(1e)^{-1}$ and $(2t_2)^{-1}$ bands of As_4. The three peaks underneath the $(2t_2)^{-1}$ band indicate the three components in this band. They are three voigt functions used to fit the band.

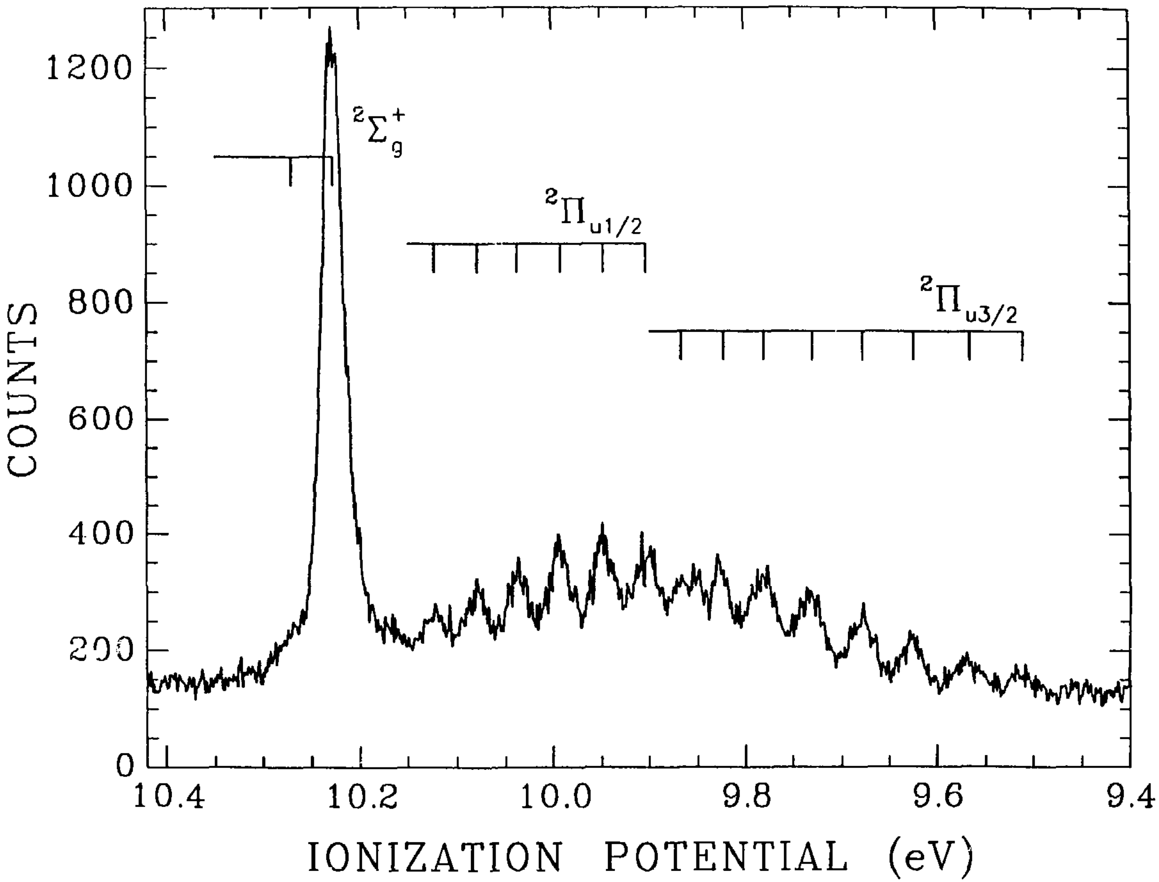
1200
1000
800
600
400
200
0
COUNTS
10.4
10.2
10.0
9.8
9.6
9.4
IONIZATION POTENTIAL (eV)
$^2\Sigma_g^+$
$^2\Pi_{u1/2}$
$^2\Pi_{u3/2}$

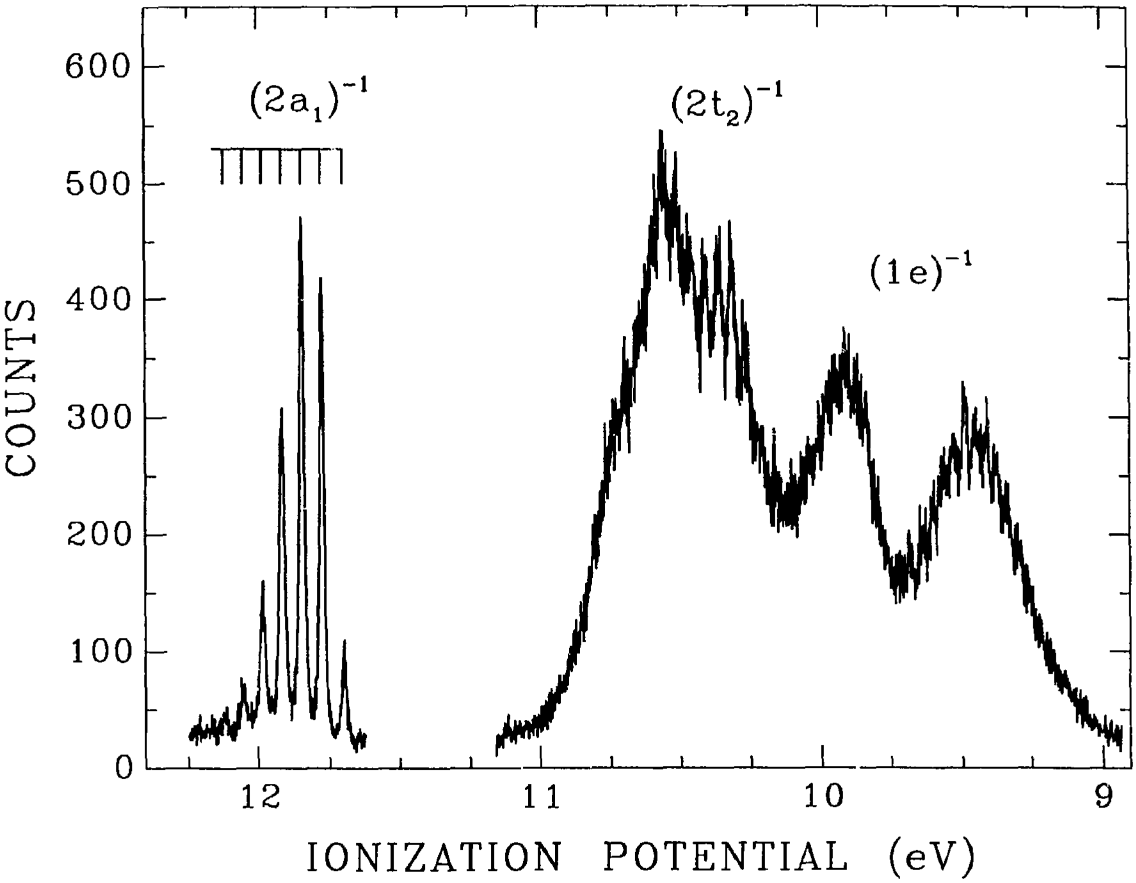
$(2a_1)^{-1}$
$(2t_2)^{-1}$
$(1e)^{-1}$
COUNTS
0
100
200
300
400
500
600
12
11
10
9
IONIZATION POTENTIAL (eV)

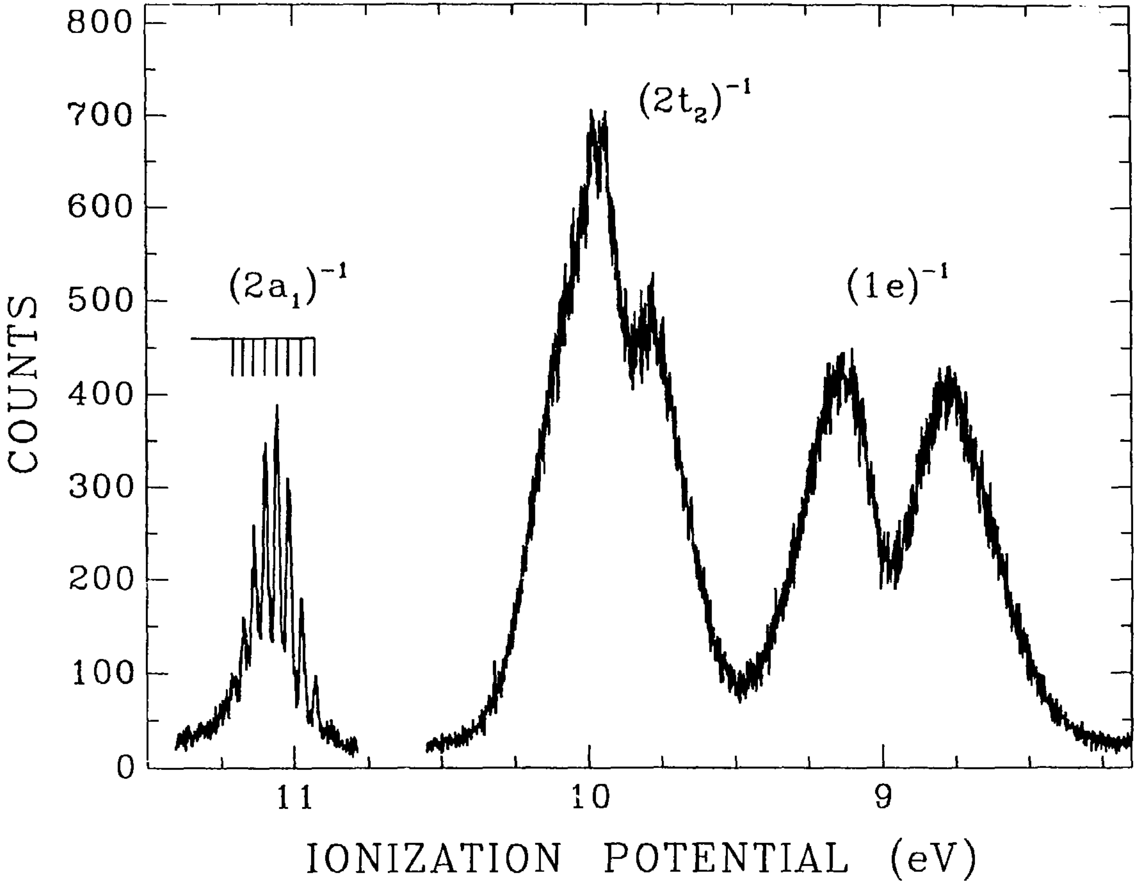
$(2t_2)^{-1}$
$(2a_1)^{-1}$
$(1e)^{-1}$
COUNTS
0
100
200
300
400
500
600
700
800
11
10
9
IONIZATION POTENTIAL (eV)

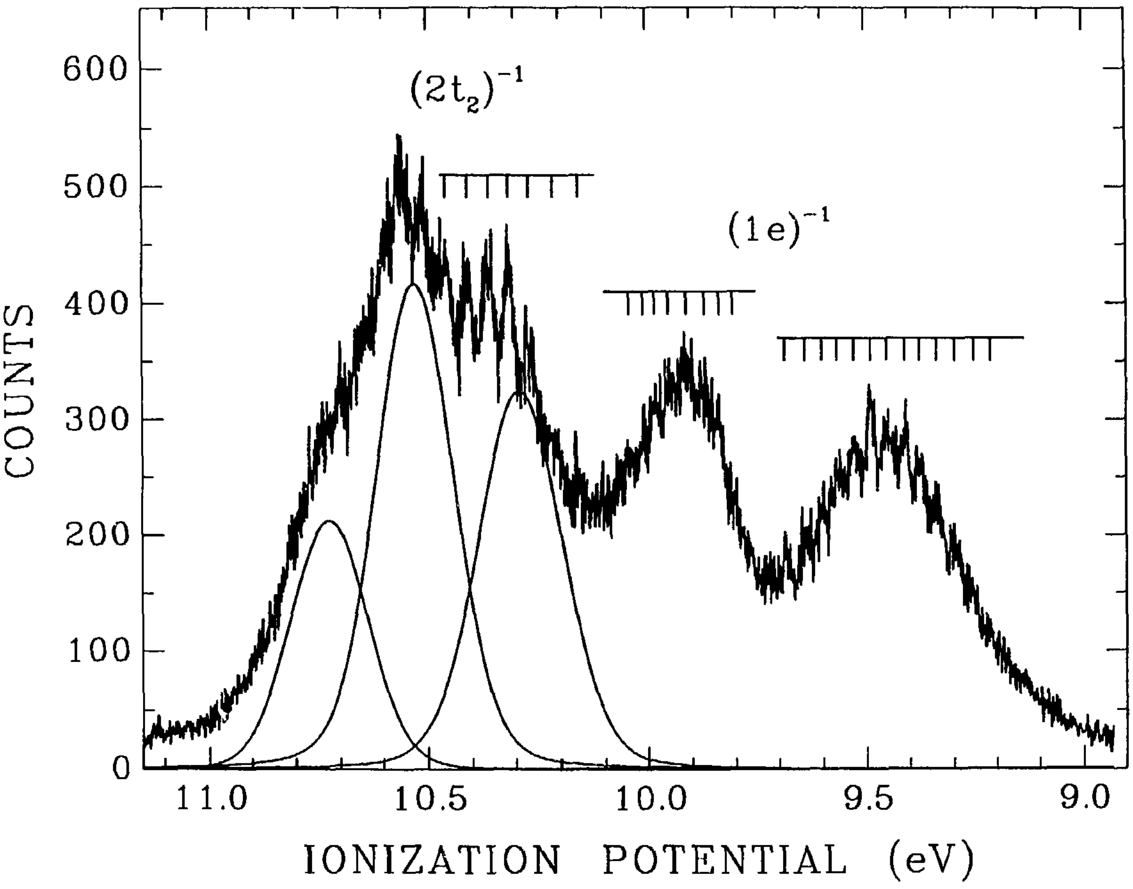
(2t$_2$)$^{-1}$
(1e)$^{-1}$
COUNTS
0
100
200
300
400
500
600
11.0
10.5
10.0
9.5
9.0
IONIZATION POTENTIAL (eV)

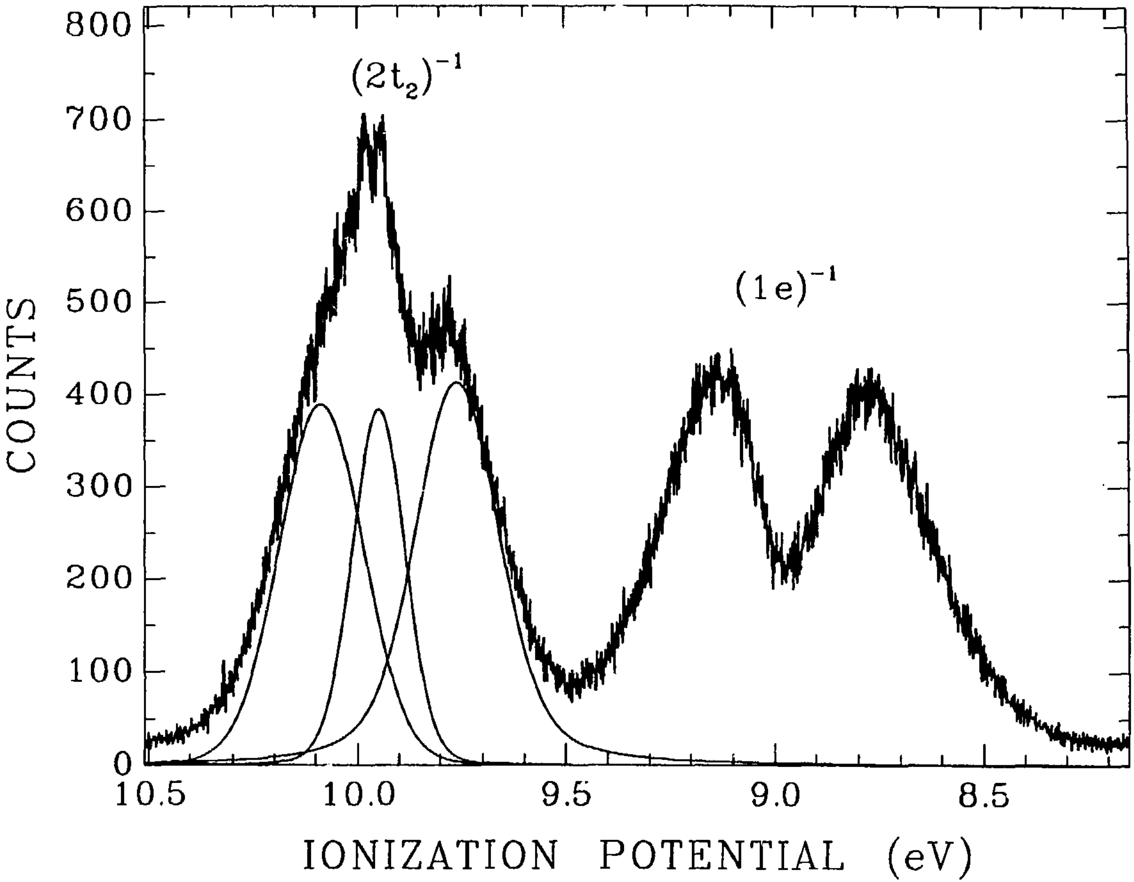
$(2t_2)^{-1}$
$(1e)^{-1}$
COUNTS
0
100
200
300
400
500
600
700
800
10.5
10.0
9.5
9.0
8.5
IONIZATION POTENTIAL (eV)